

Photophysical behavior of a homologous series of amphiphilic hemicyanine dyes in thin AOT films

L.K. Gallos^a, E. Stathatos^b, P. Lianos^b, P. Argyrakis^{a,*}

^a Department of Physics, University of Thessaloniki, 54006 Thessaloniki, Greece

^b School of Engineering, University of Patras, 26500 Patras, Greece

Received 9 May 2001; in final form 22 September 2001

Abstract

The photophysical behavior of a homologous series of amphiphilic hemicyanines, incorporated in thin films, made by dip-coating glass slides in bis(2-ethylhexyl)sulfosuccinate sodium salt (AOT) reverse micellar solutions, has been studied by absorption spectrophotometry and computer simulation techniques. At relatively high dye concentration, a narrow band in the absorption spectrum was observed, corresponding to aggregated species. Aggregates are of the H-type, displaying a hypsochromic shift in their absorption spectra, except for the shortest chain homolog. The growth of aggregates in films has been studied in relation with the [water]/[dye] and the [surfactant]/[dye] ratios. Simulation of the aggregate formation by extended dipole interaction in spherical reverse micelles and planar bilayer structures in combination with experimental data, revealed that the films are structured in microheterogeneous assemblies analogous to the reverse micelles found in the original solutions. © 2002 Elsevier Science B.V. All rights reserved.

1. Introduction

The properties of amphiphilic hemicyanine dyes is a subject of substantial investigations because of their possible applications in optoelectronics and molecular electronic devices [1,2]. Their tendency to aggregate [3,4] has been analyzed in Langmuir–Blodgett films and monolayers at the air–water interface in order to produce materials with non-linear optical properties [5,6]. Dye aggregates are also of particular importance for photographic process and xerographic reproduction as spectral

sensitizers [7]. In addition to such applications, surfactant hemicyanines, with both dyeing and amphiphilic properties are suitable components for studying photophysical phenomena such as J- and H-aggregate formation [8].

Since these dyes have a strong tendency to aggregate it is necessary to understand the nature of aggregate formation in order to fabricate assemblies with controllable properties. Here, we report an investigation on aggregate formation of the hemicyanine dyes *N*-*n*-alkyl-4-(((dimethylamino)phenyl)ethyl)pyridinium bromide, abbreviated as H*n*Hc, ($2 \leq n \leq 10$) in thin AOT surfactant films. Dye concentration in such films can achieve relatively high levels. For future application of such systems, it is then necessary to know their

* Corresponding author.

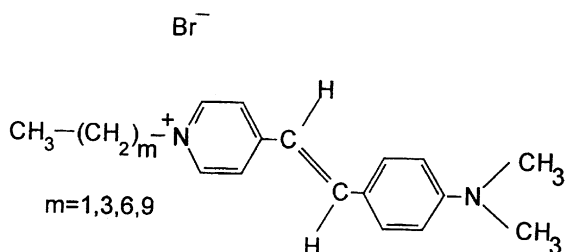
E-mail address: panos@physics.auth.gr (P. Argyrakis).

spectroscopic behavior. AOT films promptly form on glass or quartz slides when dipping in solution of AOT in cyclohexane both in the presence and in the absence of water (i.e. of reverse micelles) [9]. Such films make excellent transparent hosts for photophysical studies. These favorable properties of AOT films might make them compatible or even better than other materials used as host of dyes of optoelectronic importance.

In this work, after reviewing the solvatochromic behavior of amphiphilic hemicyanine dyes in pure solvents with different polarity, in order to have a better conception of their properties in thin films [10–12], we show the influence of water and AOT concentration on the physical state of the dyes in the films, by monitoring the absorbance of the films, in order to achieve controllable preparation procedures. Finally, we present computer simulations of different molecular configurations, which help us identify the most favorable arrangement by comparing the computed eigenenergies to the experimental absorption spectrum.

2. Experimental

Organic solvents and bis(2-ethylhexyl)sulfosuccinate sodium salt, AOT (Fluka) were of the best quality available and used as received. The hemicyanine dyes *N-n*-alkyl-4(((dimethylamino)phenyl)ethenyl)pyridinium bromide (*HnHC*) were synthesized by condensation of the corresponding *N*-alkylated 4-methylpyridines with 4-dimethylamino benzaldehyde [13]. The products were purified by repeated recrystallization from ethanol. The chemical structure of the dyes is shown here:



Films were deposited on fused silica slides by dip coating in cyclohexane solution containing reverse micelles of AOT where the dye was also solubi-

lized. The withdrawal of the slide was done at a speed of 4 cm/min. Thin orange, visibly uniform, films were formed and they were stable for several weeks. The slides were previously carefully cleaned in sulfochromic solution and rinsed with Millipore water. All preparations and measurements were made at room temperature. Absorption spectra (in the transmission mode) were recorded with a Cary 1E spectrophotometer. Fluorescence spectra (in the reflection mode) were recorded with a home-made spectrometer using Oriel parts.

3. Results and discussion

3.1. Typical absorption and fluorescence spectra in thin surfactant films

The spectroscopic behavior of hemicyanine homologs in thin AOT films requires some knowledge about their solvatochromic effect in pure solvents. A study of the dyes dissolved in various solvents has been reported in Ref. [12], where it was concluded that increasing the solvent polarity leads to a blue shift in absorption and a red shift in fluorescence [10,11,14,15].

Measurements were then made with films in the following manner: 0.07 M AOT was dissolved in cyclohexane in the presence of 0.4 M water. The dye was solubilized in the reverse-micellar solution at concentration 0.01 M. Orange-colored films were then formed on slides by dip coating. Absorption spectra of the above films are shown in Fig. 1. We attribute the maxima at 390 nm to the contribution from aggregated hemicyanine species (H-aggregate formation) and the 450 nm maxima are assigned to the monomers. Judging from the spectra of the dyes in solution, we conclude that the monomer chromophore is situated in the strongly polar environment provided by the anionic polar heads of AOT molecules. We further believe that the absorption at 450 nm is additionally the result of an ionic adduct between AOT and *HnHC* molecules [16]. H-aggregates correspond to repulsive interaction between aggregating dipoles [17], in the sense that dipole moments of the interacting dipoles are approximately pointing to the same direction. Forces of other physical origin,

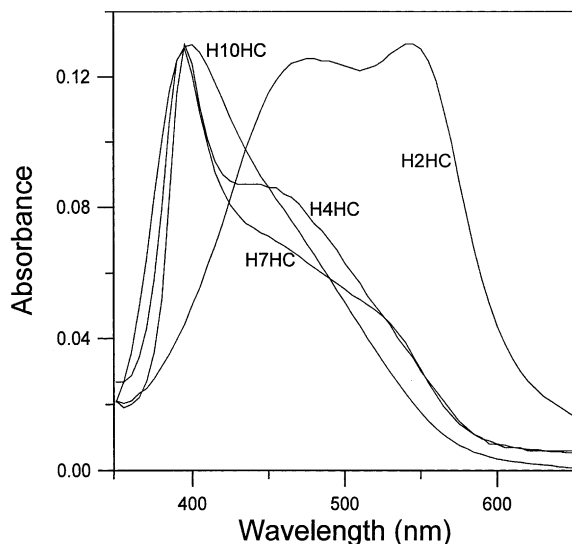


Fig. 1. Absorbance of hemicyanine homologs in thin AOT surfactant films. AOT concentration was in all cases 0.07 M while $[\text{water}]/[\text{AOT}] = 5.7$ and $[\text{dye}]/[\text{AOT}] = 1/7$.

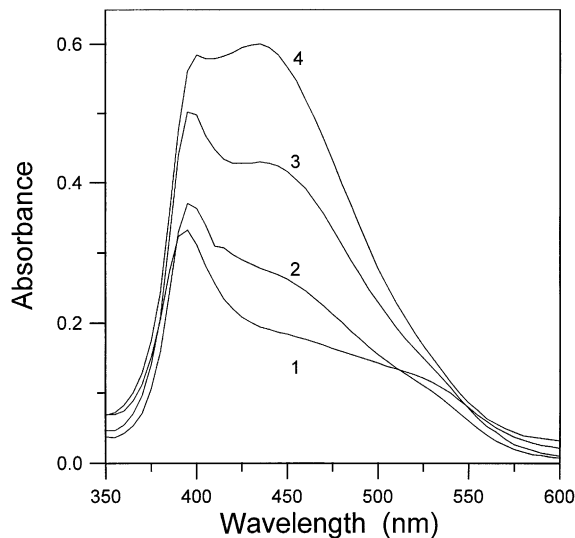


Fig. 2. Absorption of H7HC in thin surfactant films. Effect of $[\text{water}]/[\text{dye}]$ ratio on the quantity of aggregates: (1) 40, (2) 60, (3) 80 and (4) 100.

such as the hydrophobic/hydrophilic balance hold the molecules together. Thus, the degree of orientation and the extent of aggregation define the final absorbance maximum. The dyes with shorter aliphatic chains become more hydrophilic and their solubility in water increases. We expect stronger tendency toward aggregation in the case of homologs with longer aliphatic chain than those with the shorter. Indeed the homolog with two carbon atoms demonstrated a different behavior from the rest of the series. A new absorption band at 550 nm was observed and it can be assigned to rather ill-defined J-aggregates. Apparently, an aliphatic chain dictates a parallel geometry (e.g. parallel dipole moments) leading to repulsive interaction and increase of the energy of the aggregates. When the aliphatic chain is not present, attractive interaction is facilitated, leading to red shift in absorption.

3.2. Aggregation behavior with variation of critical parameters

Further studies of the aggregation process of the dyes was carried out by variation of the component relative concentrations. Fig. 2 shows the

variation of the absorption maximum from 450 to 390 nm resulting from a gradual decrease in the $[\text{water}]/[\text{dye}]$ ratio. The quantity of all dyes we used in this experiment was $[\text{dye}]/[\text{AOT}] = 1/7$ ($[\text{H}n\text{HC}] = 0.01$ M, $[\text{AOT}] = 0.07$ M). The $[\text{water}]/[\text{dye}]$ ratio varied from 40 to 100 (i.e. $[\text{water}]/[\text{AOT}]$ varied from 5.7 to 14.3). As seen then in Fig. 2, the quantity of water affects aggregate formation. A larger quantity of water results in a smaller quantity of aggregates. More water in the original reverse-micellar solution, for a given surfactant concentration, means a smaller number of reverse micelles. The number of micelles N is correlated with the total volume of all water pools by the relation $N \sim A^3/V^2$ where A is the total area of the water/oil interface and it is constant for a given surfactant concentration [18]. It is then clear that the number of reverse micelles decreases rapidly with increasing V (i.e. with increasing water content). If the number of reverse micelles decreases, while the total number of dye molecules in solution remains constant, one may expect a higher probability of coexistence of more than one dye molecules in one reverse micelle and, therefore, higher probability of aggregate formation. In addition, when the number of micelles decreases,

the number of water molecules per micelle increases, so that more water may be available to hydrate not only surfactant but also dye polar head groups. It is known that up to 10 water molecules may be necessary to complete hydration of AOT polar groups, while, above this ratio, water is available to form a water pool or to hydrate additional polar species [19]. Hydrated hemicyanines are, of course, not capable of forming aggregates. These conclusions are supported by the data of Table 1. We see in this table that an increasing amount of water results in a smaller quantity of aggregates, as already explained. This result is true for the whole homologous series. However, we note that homologs with longer aliphatic chains suffer a smaller decrease in the quantity of aggregates than the shorter-chain homologs do. This fact clearly underlines the decreased solubility of the long-chain homologs in water which implies that they are not easily attracted by the water pool, preserving thus a larger quantity of aggregates. If the dye and water concentration is fixed (0.01 and 0.4 M, respectively) but the surfactant concentration is varied, a corresponding variation of the number of the reverse-micellar entities is expected. According to the above relation $N \sim A^3/V^2$, the number of reverse micelles should rapidly increase the increasing AOT concentration. This will result in a larger dispersion of monomers in solution and subsequent larger dispersion in the film, where mobility is expected to be limited. Indeed, as seen in both Fig. 3 and Table 2, no aggregates were observed at relatively high surfactant concentration. All the above results reveal that there is an analogy between the number of reverse micelles in solution

Table 1

Effect of water addition to the ratio of the two absorption maxima corresponding to aggregate/monomer species

	H2HC	H4HC	H7HC	H10HC
$\frac{[\text{water}]}{[\text{dye}]}$	Max550 Max450	Max390 Max450	Max390 Max450	Max390 Max450
40	1.26	0.83	1.92	1.20
60	0.68	0.67	0.78	1.06
80	0.63	0.63	0.60	0.93
100	0.46	0.43	0.56	0.75
[AOT] = 0.07 M		[dye] = 0.01 M		

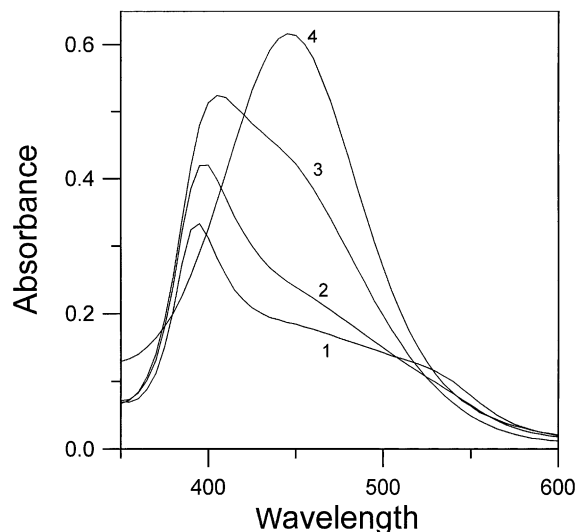


Fig. 3. Effect of [AOT]/[dye] ratio to aggregate formation of H7HC in thin films: (1) 7, (2) 10, (3) 30 and (4) 50.

and the number of separate entities forming in films, so that we believe that the reverse-micellar structure is to a large degree preserved also in films. This conclusion is in accordance with previously published findings [18,19].

3.3. Computer simulation

Based on the above, we have tried to see whether the AOT films are actually structured in separate organized molecular assemblies, analogous to the reverse micelles of the original solutions, by use of a computer simulation technique. We have

Table 2

Effect of AOT surfactant addition to the ratio of the two absorption maxima assigned to aggregate/monomer species

	H2HC	H4HC	H7HC	H10HC
$\frac{[\text{AOT}]}{[\text{dye}]}$	Max550 Max450	Max390 Max450	Max390 Max450	Max390 Max450
7	1.26	2.27	1.02	1.37
8	0.74			
10	0.34	1.19	0.86	1.16
20		0.71		
30		0.67	0.69	0.99
50			0.56	0.75
[water] = 0.4 M		[dye] = 0.01 M		

simulated the interactions between N dipoles in several conformations and chosen the one that best represents the experimental results. In what follows in the present section, we first present the theory and the model used, and then we give our results, together with related comments.

If we consider N interacting molecules, the excited states of the system can be described by the Frenkel exciton theory [20,21], where the assumption is also made that this is a two-level system (ground and excited state). The exciton matrix is formed by assigning in the diagonal elements the value of the monomer eigenenergy E_0 and in the off-diagonal elements H_{ij} the value of the interaction between the i th and the j th molecule. Diagonalization of the exciton matrix yields the N eigenenergies E_k and the corresponding eigenvectors $|k\rangle$ of the system. Each of the N eigenvectors of the system can be written as a linear combination of the unperturbed wave functions $|n\rangle$:

$$|k\rangle = \sum_{n=1}^N C_n^k |n\rangle,$$

where the coefficients C_n^k obey the normalization condition

$$\sum_{n=1}^N C_n^k C_n^l = \delta_{kl}.$$

If the transition moment dipole of a monomer is μ_{mon} the transition dipole associated to a given collective state is given by

$$\mu_k = \sum_{n=1}^N C_n^k \mu_{\text{mon}}$$

i.e. it is the vector sum of the transition dipoles for each molecule weighted by the appropriate coefficient. The oscillator strength f_k of a given state is given by

$$f_k = CE_k |\mu_k|^2,$$

where C is a constant with a value of 4.68×10^{-7} and E_k is the eigenenergy corresponding to the k th state.

In our model, the interactions are considered of dipolar nature and we use the extended dipole approximation [22] for their calculation. In this

approximation, the transition dipole moment μ is replaced by two opposite charges $+q$ and $-q$ at a distance l . Each charge feels the presence of the two charges of another dipole. Thus, the coupling between two dipoles has four terms, describing all the interactions between the charges:

$$V = q^2 \left(\frac{1}{r_{++}} + \frac{1}{r_{--}} - \frac{1}{r_{+-}} - \frac{1}{r_{-+}} \right),$$

where the corresponding distances between the positive and negative charges are denoted by r_{++} , r_{--} , r_{+-} and r_{-+} .

Since the interactions between molecules are derived mainly from their chromophore part, the dipole charges are restricted in this part and the aliphatic chain does not influence the dipole length, $l = 6.5 \text{ \AA}$, which we consider to be constant. This value of the dipole length was chosen based on the length of the chromophore part, a plausible assumption. The dipole moment is equal to $\mu = 13.8 \text{ D}$ [14,17], and we can also compute the charge q of the dipole via the relation $\mu = ql$. The diagonal terms of the exciton matrix are set equal to $E_0 = 450 \text{ nm}$, which corresponds to the monomer energy. We then form and diagonalize the exciton matrix. By diagonalizing the exciton matrix we acquire the eigenenergies and their corresponding oscillator strength. Each energy E_k is resulting in a gaussian curve centered at E_k , with a standard deviation $\sigma = 20 \text{ nm}$ and a height proportional to the oscillator strength f_k . The sum of all these gaussians yields the absorption spectrum. In the case of a reverse micelle the dipoles are located perpendicularly on the surface of a sphere whose radius R is a parameter of the model. Due to the repulsive intermolecular forces, the molecules, although restricted on this surface, tend to lie as far apart from each other as possible. The problem of positioning N points on the surface of a three-dimensional sphere so that the smallest distance between any pair is maximized is known as the Tammes problem. The exact solution is known only for $N < 13$ and $N = 24$ [23]. We have also tried $N = 60$ by utilizing the structure of fullerenes (C_{60}), which is a stable form of carbon, and provides us with a minimum energy configuration.

First, we examined the case of a layer arrangement. The molecules were placed on a square

lattice. The lattice grid was comprised by 20×20 sites, and the lattice spacing was a free parameter. The molecules were placed so that they were parallel to each other and their long axes were pointing normal to the lattice. For lattice spacing in the range 10–20 Å the procedure described above yields only one distinguishable peak with an elongated tail at the red part of the spectrum. The experimental spectral shift is obtained for a lattice spacing of 12 Å, and the width of the peak can be fitted quite accurately (Fig. 4). However, this lattice conformation cannot predict the smaller peaks, which form the shoulder of the experimental spectrum.

We also examined the case of a bilayer arrangement. We consider that there are two square layers on top of each other. The separation distance between them was varied and the molecules on a layer were placed opposite to the molecules of the other layer. We could see that the best fitting in terms of predicting the experimental shift is found when the layers separation was 5 Å and the lattice constant was 15 Å, but again the smaller absorption band cannot be predicted by this arrangement. We also note that the dominant peak of the simulated

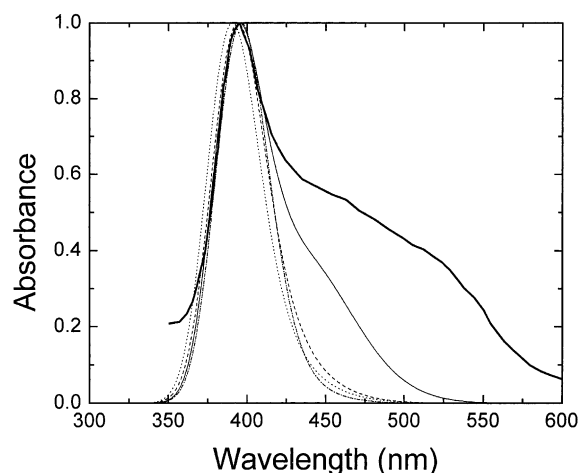


Fig. 4. Comparison of simulated absorption spectra to the experimental absorption spectrum of H7HC (thick line) in thin films. The simulated spectra of the different layer configurations described in the text are similar to each other and are represented by the dashed lines, while the continuous curve corresponds to a reverse-micelle conformation.

spectrum is not attributed to a single eigenstate, but is rather due to a certain number of collective states with nonzero oscillator strength which fall in the same energy region; because of the bandwidth assigned to each of these states their convoluted sum, which represents the final spectrum, seems to have only one band at that point. Similarly, there are many collective states with nonzero oscillator strength, but this strength is small compared to the main peak and after the convolution process they are no longer distinguishable at the final spectrum. The comparison of this spectrum to the experimental one is presented in Fig. 4.

The final layer arrangement studied was that of a multilayer, where successive chromophore layers are separated by water layers. The structure used is as follows: we consider $N \times N$ molecules on a square lattice with lattice constant a . Under this layer we place a second one, and the distance between the chromophores is equal to the carbon chain length plus a small distance h , which we consider as a free parameter, because of the chains overlap. A water layer of thickness d follows and the arrangement of the two chromophore layers is repeated below this water layer. In short, the parameters are the lattice constant a , the distance between the chains h , and the water layer thickness d , as well as the number on monomers $N \times N$ which construct each layer.

Initially, we varied the number of monomers on each layer. As we increase this number from 36 per layer to 400 per layer we observe a shift to higher energies and the existence of a secondary peak, which gradually reduces with increasing N . When we compare, for this specific configuration, the three compounds with different chain lengths we have the interesting result that there is no change in the wavelength of the peak, which is also an experimental result (Fig. 1). The best fitting was accomplished for $a = 12$ Å, $N = 15$, $h = 2$ Å and $d = 2$ Å. By also varying the values of the parameters h and d up to 5 Å we observed that the spectrum remained practically the same. We can see that although there is no distinguishable smaller peak, the tail at the red part of the spectrum is quite elongated, which shows that there are a few eigenstates that bear a small part of the oscillator strength in this energy region.

The above models were successful in predicting the experimental spectral shift but could not predict the smaller band. In fact, the desired shift can be achieved by varying the structural parameters of a model, so that the magnitude of the corresponding interactions between the chromophores yields the required peak. The smaller band, which is close to the monomer energy, should appear if the system geometry isolated in some way certain molecules from interacting with other molecules. However, the symmetry of the layer arrangements described seems not to allow states with energy close to that of a monomer to bear any important part of the oscillator strength.

Finally, we tried to simulate the spectrum of a spherical micelle. The parameters varied in this simulation are the radius R of the micelle and the number N of dipoles placed perpendicularly on the surface of this sphere. In general, the spectrum is more spread and the exciton shift increases for smaller R or larger N . Of course, this trend is expected because when we force many molecules in a small space the interaction energy is much higher than when this space is larger. So, when the molecules are spatially spread, more molecules are needed in order to yield the same energy shift. When the molecules are close to each other there are many peaks with considerable heights mainly for large energies, although red-shifted peaks are also present. As we increase the radius R the spectrum becomes narrower and progressively only one prominent peak remains. The increase of N also results in a higher blue shift and more eigenstates with nonzero oscillator strength.

If we consider that the main molecular configuration on the film is this of a micelle we can try to fit the experimental spectra to our simulation spectra. After a systematic variation of the parameters the best fit was found for $N = 60$ and $R = 21 \text{ \AA}$. Although the exact line shape cannot be accurately reproduced, one can see that the main spectral characteristics can be predicated. Thus, the location of the maximum is at the same energy level and the lower peaks appear at roughly the same energies, although their predicted height is lower.

The computer simulation data then come in support of the experimental results, i.e. that the films are structured in segregated segments that

possess the characteristics of spherical reverse micelles.

4. Conclusions

The above data demonstrate the tendency of amphiphilic hemicyanine dyes to aggregate when incorporated in thin AOT films. This aggregation behavior is translated as a strong repulsive dipole–dipole interaction, which is facilitated by the orientation factor imposed by the aliphatic chain. In this respect, longer aliphatic chains impose a higher orientation factor while short chain analogues do not demonstrate any repulsive interaction. The present data, in conjunction with previous findings [18,19], indicate that the structure of AOT thin films made from reverse-micellar solutions is compatible with the existence of separate entities corresponding to the reverse micelles of the original solution and most probably resembling. Given the fact that AOT films are easy to make, that they can be easily controlled by changing simple parameters, such as water or surfactant concentration, that they are transparent and that they can accommodate a relatively large number of dye species, they can be useful to various photophysical applications.

Acknowledgements

We are very grateful to Prof. Andre Laschewsky (Chemistry Dept., Université Catholique de Louvain, B-1348 Louvain-la-Neuve, Belgium) for providing the hemicyanine dyes and for his comments and information concerning this work. We also acknowledge financial aid from a grant by the Greek Secretariat of Research and Technology (PENED 3497/95).

References

- [1] D. Li, M.A. Ratner, T.J. Marks, C. Zhang, J. Yang, G.K. Wong, *J. Am. Chem. Soc.* 112 (1990) 7389.
- [2] D. Mobius, H. Kuhn, *J. Appl. Phys.* 64 (1988) 5134.
- [3] Q. Song, C.E. Evans, P.W. Bohn, *J. Phys. Chem.* 97 (1993) 12302.

- [4] Q. Song, C.E. Evans, P.W. Bohn, *J. Phys. Chem.* 97 (1993) 13736.
- [5] B.L. Anderson, J.M. Hoover, G.A. Lindsay, B.G. Higgins, P. Stroeve, S.T. Kowel, *Thin Solid Films* 179 (1989) 413.
- [6] K. Kajikawa, H. Takezoe, A. Fukuda, *Jpn. J. Appl. Phys.* 30 (1991) 1050.
- [7] Y.S. Kim, K. Liang, K.Y. Law, D.G. Whitten, *J. Phys. Chem.* 98 (1994) 984.
- [8] S. Ma, X. Lu, J. Song, L. Liu, W. Peng, J. Zhou, Z. Yu, W. Wang, Z. Zhang, *Langmuir* 11 (1995) 2751.
- [9] D. Papoutsis, V. Bekiari, E. Stathatos, P. Lianos, A. Laschewsky, *Langmuir* 11 (1995) 4355.
- [10] H. Ephardt, P. Fromherz, *J. Phys. Chem.* 93 (1989) 7717.
- [11] H. Ephardt, P. Fromherz, *J. Phys. Chem.* 97 (1993) 4540.
- [12] E. Stathatos, P. Lianos, A. Laschewsky, *Langmuir* 13 (1997) 259.
- [13] K. Lunkenheimer, A. Laschewsky, *Prog. Coll. Polym. Sci.* 89 (1992) 239.
- [14] P. Fromherz, *J. Phys. Chem.* 99 (1995) 7188.
- [15] M.L. Loew, L. Simpson, A. Hassner, V. Alexanian, *J. Am. Chem. Soc.* 101 (1979) 5439.
- [16] M. Hof, P. Lianos, A. Laschewsky, *Langmuir* 13 (1997) 2181.
- [17] C.E. Evans, P.W. Bohn, *J. Am. Chem. Soc.* 115 (1993) 3306.
- [18] V. Bekiari, P. Lianos, *J. Coll. Interf. Sci.* 183 (1996) 552.
- [19] M. Hof, P. Lianos, *Langmuir* 13 (1997) 290.
- [20] J. Frenkel, *Phys. Rev.* 37 (1931) 1276.
- [21] A.S. Davydov, *Theory of Molecular Excitons*, Plenum Press, New York, 1971.
- [22] V. Czikkleky, H.D. Fosterling, H. Kuhn, *Chem. Phys. Lett.* 6 (1970) 207.
- [23] B.W. Clare, D.L. Kepert, *Proc. Roy. Soc London Ser. A* 405 (1986) 329.